

PAPER • OPEN ACCESS

Tensile strength of Al matrix with nanoscale Cu, Ti and Mg inclusions

To cite this article: V V Pogorelko and A E Mayer 2016 *J. Phys.: Conf. Ser.* **774** 012034

View the [article online](#) for updates and enhancements.

You may also like

- [Microelectrochemical Properties of Ti\(C,N\) Inclusion of High Strength Martensitic Carbon Steel](#)

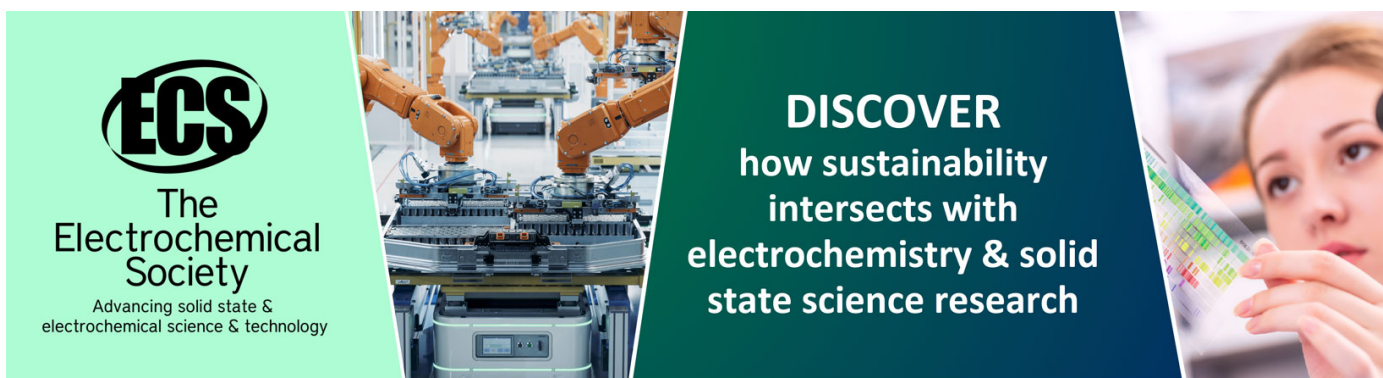
Yuta Watanabe, Izumi Muto, Tomohiko Ohmura et al.

- [Beneficial Effects of Cerium Addition to Sulfide Inclusions on Pitting Corrosion Resistance of Stainless Steels](#)

Masashi Nishimoto, Izumi Muto, Yu Sugawara et al.

- [Microscopic Polarization Behavior of Cerium Sulfide Inclusions in Stainless Steel](#)

Masashi Nishimoto, Izumi Muto, Yu Sugawara et al.



ECS
The
Electrochemical
Society
Advancing solid state &
electrochemical science & technology

DISCOVER
how sustainability
intersects with
electrochemistry & solid
state science research

Tensile strength of Al matrix with nanoscale Cu, Ti and Mg inclusions

V V Pogorelko and A E Mayer

Chelyabinsk State University, Bratiev Kashirinykh Street 129, Chelyabinsk 454001, Russia

E-mail: vik_ko83@mail.ru

Abstract. Molecular-dynamic investigations of Al+Cu, Al+Ti and Al+Mg nanocomposite strength under high-rate uniaxial tension were carried out in this work. We consider two different mechanisms of reduction of the tensile strength of a material with inclusions in comparison with a pure material of matrix. The first mechanism is connected with a stress concentration in matrix near a stiff and strong inclusion (Ti, Cu); in this case, the fracture occurs inside the matrix and does not touch the inclusion. The second mechanism acts in the case of a soft and weak inclusion (Mg); the fracture begins inside the inclusion and thereafter propagates into the matrix. The tensile strength of the systems is determined at varied strain rates (in the range from 0.1/ns to 30/ns at the temperature 300 K) and varied temperatures (in the range from 300 K to 900 K at the strain rate 1/ns).

1. Introduction

At the present time nanocomposites [1], and alloys [2] with aluminum matrix are widely used in various applications. They can have better properties (stiffness, specific shear strength, etc.) in comparison with a pure material of matrix. Heterogeneity is a common feature of alloys and nanocomposites. The presence of nanoinclusions in matrix obstructs the motion of dislocations that leads to an increase of shear strength [3]. On the other hand, the presence of inclusions [4] can decrease the tensile strength. For ascertainment of the mechanisms and regularities and for estimation the degree of influence of the inclusions on the strength, a molecular-dynamics (MD) investigation of Al+Cu, Al+Ti and Al+Mg composites fracture under the high rate tension was carried out in this work. The MD data were generalized by construction of a continuum model of fracture. The results may be useful for analysis of the strength of aluminum alloys with the precipitates of the second phase.

2. MD setup

MD simulations were performed using the parallel MD simulator LAMMPS [5] with interatomic potentials [6], [7] and [8] for the cases of Ti, Mg and Cu inclusions, respectively; these potentials were based on the formalism of the embedded atom method (EAM) [9].

We considered samples of pure Al and aluminum with spherical inclusions made of α -Ti, Mg and Cu. In all cases, we initially specify a sample of monocrystalline aluminum (fcc lattice) of cubic shape (with a cube face length denoted as d), which was oriented in such a manner that the lattice directions [100], [010] and [001] coincides with the cube faces (with the coordinate axes x , y and z). A sphere with a specified radius R was cut out from the center of the system (Al



cube), thereafter, a sphere of monocrystalline copper (fcc lattice) magnesium or titanium (hcp lattices) of the same radius was placed inside the pore. Lattice of Cu inclusion was oriented in such a way that the lattices directions [100], [010] and [001] coincide with the cube faces similar to the matrix. A standard hcp lattice was specified for α -Ti and Mg; orientation of the lattice relative to the coordinate system (cube faces): x axis coincided with the lattice direction $[2\bar{1}\bar{1}0]$, y axis was directed along $[01\bar{1}0]$, and z axis was directed along $[0001]$. Overlapping of atoms was not observed in all investigated cases; at the same time, the contact between atoms of inclusions and surrounding matrix was fine, which was confirmed by additional simulations with an energy minimization procedure after the inclusion insertion: results with this additional procedure and without this procedure coincided with each other.

Periodic boundary conditions were set for all boundaries of MD sample that is equivalent to consideration of a system of identical, periodically arranged inclusions with concentration d^{-3} ; volume fraction of inclusions is equal to $(4\pi/3)(R/d)^3$. For the cases of pure aluminum and aluminum with inclusions, all calculations were performed for a system with the size $50 \times 50 \times 50$ of the lattice parameters of aluminum that corresponded to initial length of the cube face of about $d = 20$ nm, and the number of atoms in the model was about 500 000. Systems with a similar number of atoms were investigated in the case of pure α -Ti and Mg. The initial radius of inclusions R was equal to 10 lattice parameters of aluminum (about 4 nm, diameter was about 8 nm) that corresponds to the volume fraction of inclusions of about 0.034.

A uniform uniaxial tension with a constant strain rate was modeled with using the “deform” command of LAMMPS that corresponds to the substance expansion under its own inertia. This type of deformation is realized under the action of a plane unloading wave on material, for instance. The system was deformed in a Nose–Hoover thermostat at the constant temperature and with the relaxation time of 0.1 ps (time step was 0.001 ps). Prior to deformation, the system was brought to thermodynamic equilibrium at the given temperature and atmospheric pressure during 100 ps; the Nose–Hoover thermostat and barostat were used at this stage.

In order to take account of non-ideality of the real structures of alloys and composite materials, we did similar computations with nanocrystalline aluminum. Samples with the grain boundaries were prepared by modelling metal melt crystallization process on several disoriented crystallization centers placed randomly into the overcooled melt. As a result, nanosized grains with a typical size of 10 nm and a thickness of the grain boundary of 3-5 interatomic distances were formed. Fraction of the grain boundaries in the nanocrystalline aluminum was about 0.1. Based on the derived nanocrystalline aluminum and method described above, composites with inclusions of the copper and magnesium were prepared.

3. Results and discussion

3.1. Monocrystalline aluminum with inclusions

Investigations of Al+Cu composite strength were performed in [4]. Figure 1 shows the time dependences of pressure in pure aluminum and Al+Cu composite. A monotonic decrease of pressure takes place at the initial stage of tension; the curves for pure aluminum and composite are practically identical at this stage that indicates the close values of elastic moduli of materials. Initially, the deformation of the material is elastic with maintaining the order of the atoms. When reaching the negative pressure of a critical value (dynamic strength), the fracture of material begins, which manifests itself in the formation and growth of voids. The material between the voids is compressed, which leads to a sharp removal of tensile stress (pressure grows). We are primarily interested in the value of the dynamic tensile strength. The presence of copper inclusions in aluminum reduces this value (figure 1). Additional calculations have shown that the influence of the radius of the copper inclusions on the tensile strength of system Al+Cu is small. For example, changing the radius of copper inclusion from 5 to 20 periods of the lattice leads to a change in the strength of less than 5%.

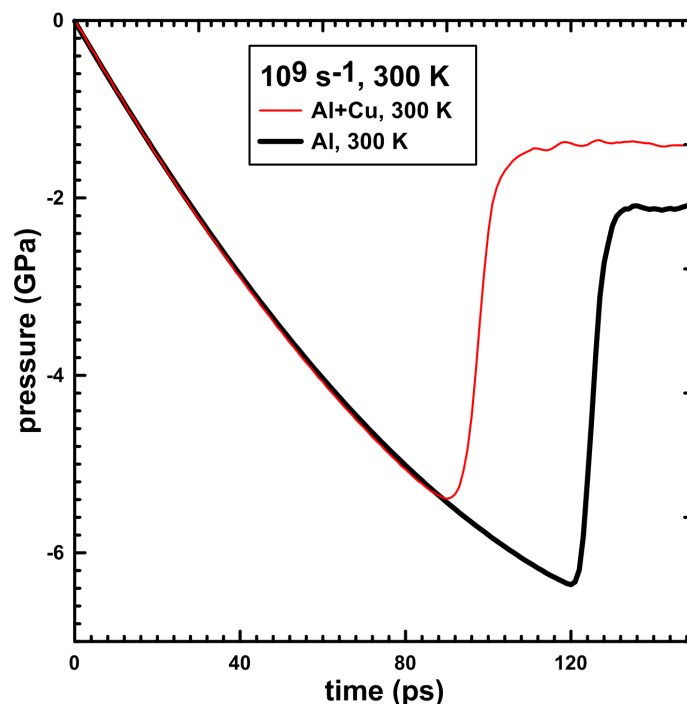


Figure 1. The time dependences of pressure in pure aluminum and composite materials. Strain rate is 10^9 s^{-1} . Calculations with the interatomic potential [8].

In a homogeneous material, the voids arise in random locations of the computational domain. At the presence of inclusions, formation of a void occurs in the aluminum matrix, and its position is correlated with the position of inclusion. The void growth dynamics at the material temperature of 300 K is shown in figure 2. The figure shows the distribution of centrosymmetric parameter illustrating violation of the crystal structure; these violations are associated with the boundary of inclusion, traces of dislocation glide and the surface of the void. Program OVITO [10] was used for visualization. At the temperatures $\leq 700 \text{ K}$, a scenario of void formation is the same and similar to that shown in figure 2. Voids formation occurs in the aluminum matrix near the surface of the inclusion directly below or above the inclusion (figure 2), if the direction of tension is conditionally accepted as vertical direction. At the same time, several atomic layers of aluminum remain on the copper inclusion, which indicates good adhesion properties of such a system. Formation of void is preceded by formation of dislocations in the corresponding region near the interface; the dislocations form a branched structure in aluminum, but do not penetrate into the copper inclusion with rare exceptions. The void growth is provided by plastic deformation due to the motion of dislocations in its neighborhood that is a viscous growth; embrittlement of the material does not take place.

The reasons for the observed behavior of the system are clear from the pressure distributions in the aluminum matrix around the inclusion. Since the elastic moduli of copper are greater than that of aluminum, a higher tensile stress acts in the interior of the copper inclusions in comparison with the volume-average value to ensure the compatibility of strains. This leads to a redistribution of stresses in the adjacent layers of aluminum matrix and the appearance of stress concentrators. Thus, under the considered conditions of loading, the stress concentration on copper inclusions is the main reason for the decrease in tensile strength of nanocomposite compared with pure aluminum.

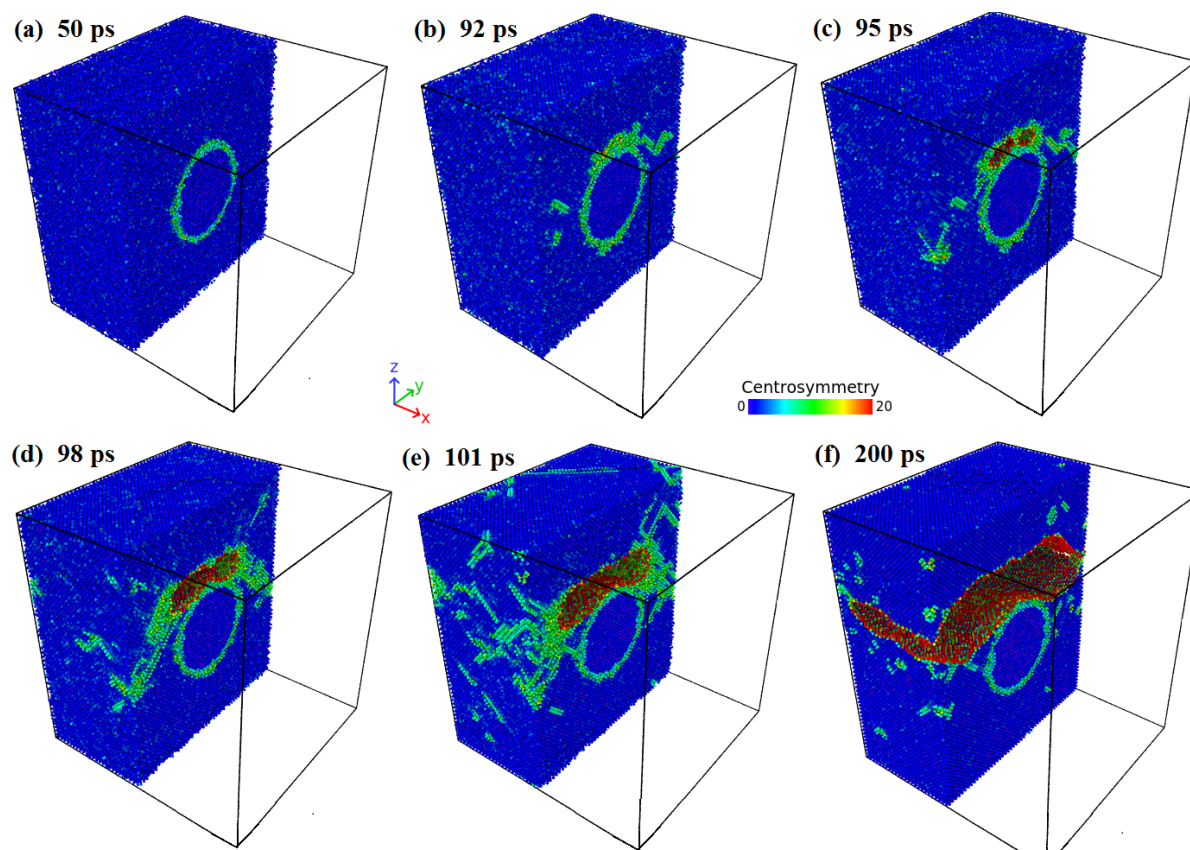


Figure 2. Distributions of centrosymmetric parameter in subsequent moments of time: tension of Al+Cu at the strain rate of 10^9 s^{-1} and temperature of 300 K. Calculations with interatomic potential [8]. Tension is along vertical direction.

Figure 3 presents the time profiles of pressure in the MD systems of pure Al and Ti, as well as Al matrix with Ti inclusions, at the stage of tension. Tension was simulated along all coordinate axes in the cases of Ti and Al+Ti systems due to anisotropy of α -Ti. In the case of pure Ti, there is a strong dependence on the tension direction: tensions along x and y axes give close results, while deformation along z axis is characterized by a higher dynamic tensile strength and a smaller curve slope at the initial stage of elastic deformation that is determined by the elastic constants. In the case of pure Al, the initial slope of deformation curve (it means, the elastic constants) and the tensile strength are less than the corresponding values in the case of pure Ti. Aluminum with Ti inclusions has even less tensile strength, and the minimal strength corresponds to the tension along z axis. For Al+Ti system, the change of strength with variation of the tension direction is substantially less than in the case of pure Ti. Curves for Al+Ti system coincide with the curve for pure Al till the beginning of fracture; this fact evidences a weak influence of inclusions (with the volume fraction of about 0.034) on the elastic properties of the system as a whole.

The dynamics of fracture development in Al+Ti system is illustrated in figure 4, which consequently shows the atoms of inclusion and the atoms of matrix with violations of crystal lattice in their vicinity. There are no appreciable defects inside the Al lattice during the initial stage of deformation. A void appears above the inclusion (we conditionally consider the tension direction, along z axis, as a vertical one) at time of 80 ps and starts to grow: one can see Al

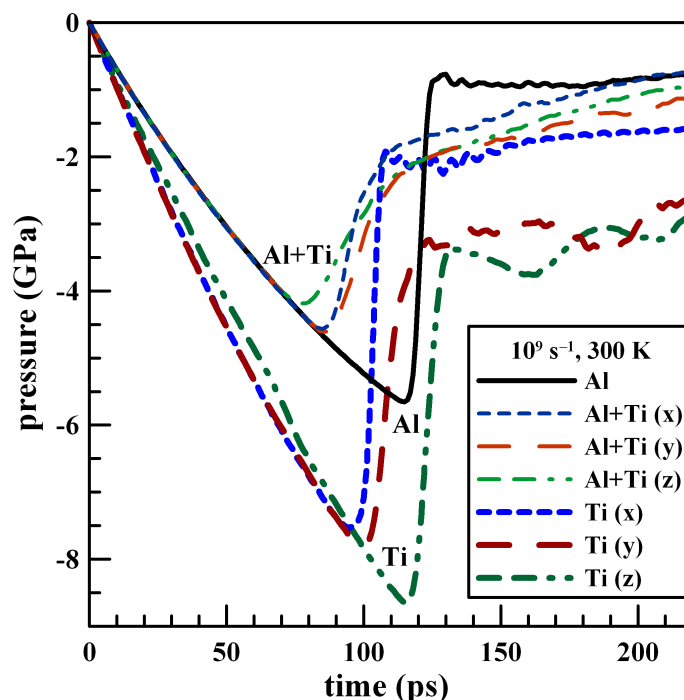


Figure 3. Time profiles of pressure in pure aluminum (“Al”), titanium (“Ti (x)”, “Ti (y)” and “Ti (z)”), and Al matrix with Ti inclusions (“Al+Ti (x)”, “Al+Ti (y)” and “Al+Ti (z)”): uniaxial tension with the constant strain rate of 10^9 s^{-1} at the constant temperature of 300 K. Simulation results of tension along each axis are presented for pure Ti and Al+Ti system.

atoms on the surface of this void in figure 4 for the corresponding instants of time. The moment of void formation correlates with the achievement of the minimal value of pressure in the system (figure 3). Initial shape of the void is close to a spherical one; subsequent deformation leads to predominant growth in directions that are perpendicular to the direction of tension. The void reaches the boundaries of MD system at time of 150 ps (figure 4); due to the using of the periodic boundary conditions, it corresponds to a coalescence of adjacent voids in main cracks that leads to the material fragmentation on layers, which are perpendicular to the tension direction. This coalescence is the final stage of fracture, but material loses its strength substantially earlier—at reaching the minimal pressure.

The void grows purely inside the Al matrix and does not touch the Ti inclusion. Though the void nucleation occurs near the inclusion, several atomic layers of Al remain on the inclusion surface that indicates a good adhesion of Al and Ti atoms and absence of a delamination along the interface. Thus, similar to the case of Cu inclusions, the mechanism of reduction of the tensile strength consists in the stress concentration in the matrix near the inclusions.

Figure 5 presents the time profiles of pressure in the MD systems of pure Al and Mg, as well as Al matrix with Mg inclusions, at the stage of tension; in the last two cases, the tension was simulated along all coordinate axes. Similar to α -Ti, there is a strong dependence on the tension direction in the case of pure Mg: tensions along x and y axes give close results, while deformation along z axis is characterized by a substantially lower tensile strength and a larger curve slope at the initial stage of elastic deformation that is determined by the elastic constants. Initial slope of deformation curve (it means, the elastic constants) and the tensile strength of pure Al are more than the corresponding values in the case of pure Mg. Aluminum with Mg inclusions has

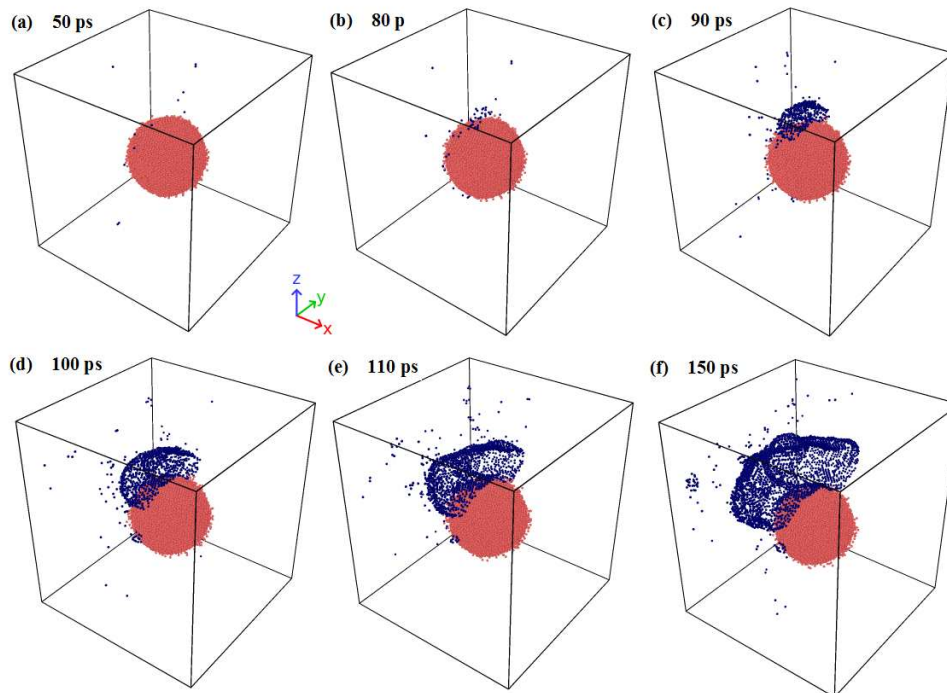


Figure 4. Dynamics of void growth in Al matrix above Ti inclusion; the temperature is 300 K, and the strain rate is 10^9 s^{-1} . Light red dots show Ti atoms; dark blue dots show Al atoms with the value of the centrosymmetric parameter (for fcc lattice) more than 17 (atoms in vicinity of lattice defects) and with coordinate $x \leq L_x/2$, where L_x is the size of MD system along x axis (in the faraway half of MD system). Parallelepiped shows the boundaries of MD system.

an intermediate value of tensile strength, and change of the tension direction leads to a weak variation of strength of this system. A close slopes of initial pieces of the deformation curves for Al and Al+Mg systems evidences a weak influence of inclusions on the elastic properties of the system as a whole, similar to the case of Ti inclusions.

Figure 6 shows the dynamics of fracture development in the Al+Mg system. The fracture starts inside the Mg inclusion in this case. A tendency to formation of two voids is observed initially (figure 6b); one of these voids becomes dominant one (figures 6c, 6d). Growth of the dominant void relaxes the stresses inside the inclusion that, particularly, suppresses the growth of the second void. The void growth inside the inclusion is accompanied by plastic flow and formation of lattice defects in the surrounding Al matrix (figures 6c, 6d). Size of the dominant void reaches the size of inclusion, and the void disrupts the inclusion (figure 6e); thereafter, the void penetrates inside the Al matrix and grows in directions that are perpendicular to the direction of tension (figure 6f) till the complete fracture and fragmentation of the material.

The Al matrix is stiffer than the Mg inclusion; therefore, lesser stresses are applied to inclusion than that to the matrix in order to provide the strain compatibility. The decreased stresses inside the inclusion explain the fact that the fracture in Al+Mg system starts at higher average stresses than in the case of pure Mg.

Figure 7 collects the results of investigations of the tensile strength of the Al+Ti and Al+Mg systems at the temperature of 300 K in the range of the strain rates from 10^8 s^{-1} to $3 \times 10^{10} \text{ s}^{-1}$. Each point that is shown by symbol is calculated by averaging of several (from 4 to 6) MD trajectories, the corresponding error ranges that characterize the statistical straggling of results

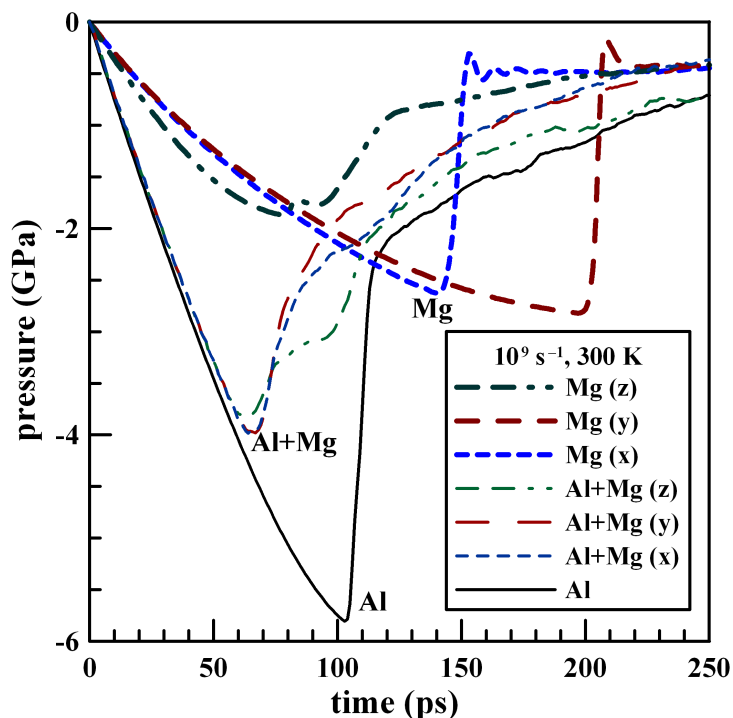


Figure 5. Time profiles of pressure in pure aluminum (“Al”), magnesium (“Mg (x)”, “Mg (y)” and “Mg (z)”), and Al matrix with Mg inclusions (“Al+Mg (x)”, “Al+ Mg (y)” and “Al+ Mg (z)”): uniaxial tension with the constant strain rate of 10^9 s^{-1} at the constant temperature of 300 K. Results of tension along each axis are presented for pure Mg and Al+Mg system.

are also shown. In all cases, the tensile strength of Al with inclusions is less than that for pure aluminum. Cu inclusions lead to the least decrease of the strength among others (with taking into account the difference in strength values of pure Al that are calculated with using various potentials [6], [7] and [8]), Ti inclusions lead to a more strong effect, while Mg inclusions causes the maximal decrease of strength. Growth of the strain rate up to $3 \times 10^{10} \text{ s}^{-1}$ results in vanishing of difference between strengths of pure Al, Al+Cu and Al+Ti system. This change of behavior is connected with a transition from the mode of voids nucleation inside the stress concentration areas to the mode of nucleation in a whole volume of the Al matrix [4]: the higher strain rate, the larger number of voids necessary for efficient relaxation of tensile stresses, as a result, voids appears not only inside the areas of concentration, but in the rest of matrix, which requires the same negative pressure as for pure Al. There is no so distinct transition in the case of Mg inclusions, but the difference between strengths of pure Al and Al+Mg system also decreases with the strain rate increase. In general, the rate sensitivity of material with inclusions is larger than that for a pure material without inclusions; similar tendency is observed in [12], [13] for Al with pores.

Figure 8 shows the results of investigation of the temperature dependence of strength for Al+Ti and Al+Mg systems at the strain rate 10^9 s^{-1} , and the results of [4] for Al+Cu system. Temperature dependences of strength for pure Al that are calculated with using the potentials [6], [7] and [8] are presented for comparison. The potentials [6] and [8] give different values of strength of pure Al, but close curve slopes of temperature dependences. The potentials [6] and [7] give close values of strength at 300 K, but the curve slope of temperature dependence for [7] is less than that for potentials [6], [8]. Besides that, the potential [7] gives a maximum of strength

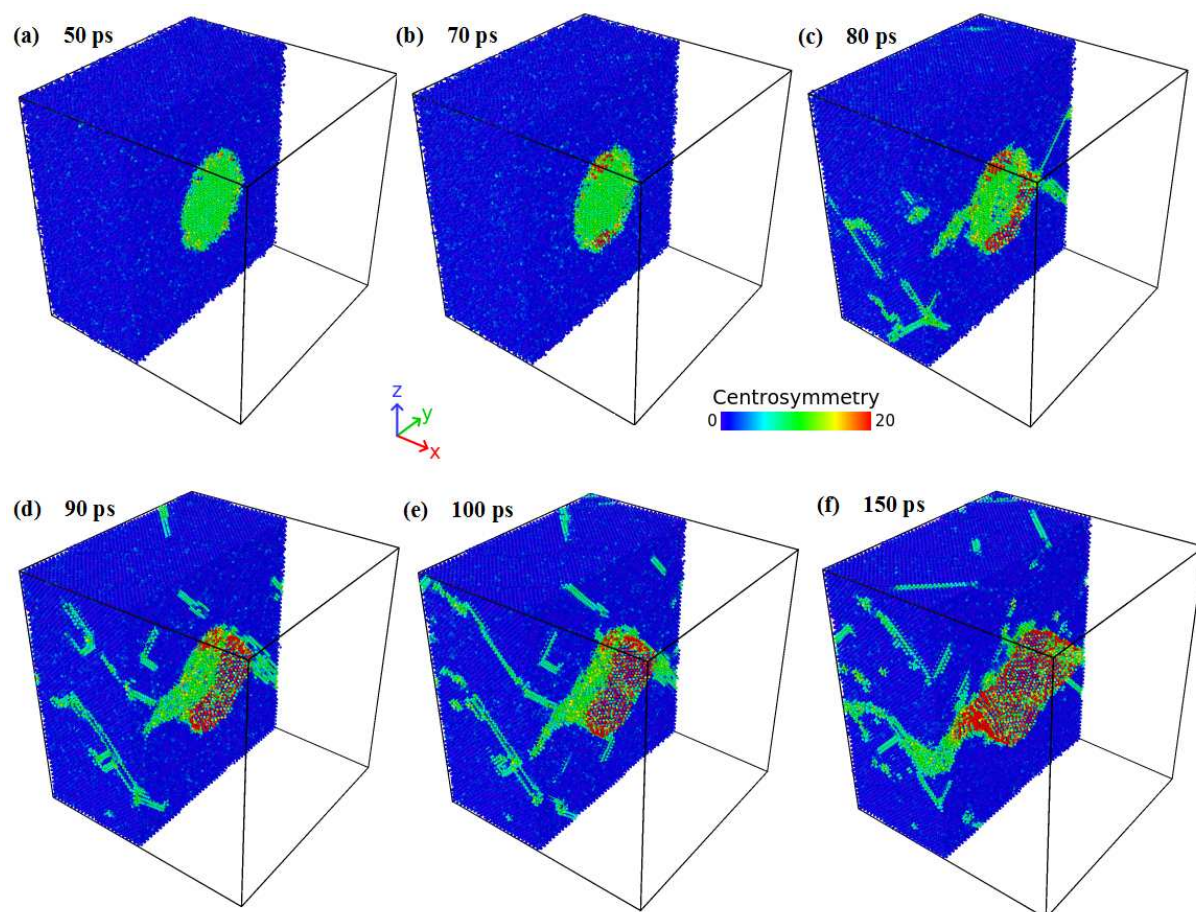


Figure 6. Dynamics of fracture of Al matrix with Mg inclusion; the temperature is 300 K, and the strain rate is 10^9 s^{-1} . Atoms are colored according to the values of centrosymmetric parameter (“Centrosymmetry”) that is calculated for fcc lattice, and, therefore, atoms of inclusion (hcp lattice) initially have a non-zero value of this parameter. Parallelepiped shows the boundaries of MD system.

at the temperature of 400 K, which is reliably registered on a large number of MD trajectories; the nature of this maximum is unclear. Therefore, the comparison of temperature dependences is qualitative one.

3.2. Nanocrystalline aluminum with inclusions

In this work we also carried out investigation of the tensile strength of nanocrystalline aluminum and of made on its basis composites with copper and magnesium inclusions. Presence of the grain boundaries in nanocrystalline aluminum reduces their tensile strength. For example, the tensile strength of nanocrystalline aluminum at strain rate 10^9 s^{-1} and at temperature 300 K calculated with using of interatomic potential [8] was 4.7 GPa (for monocrystalline aluminum with the same interatomic potential [8] was 6.4 GPa).

Figure 9-10 show the distributions of centrosymmetric parameter in subsequent moments of time for the nanocrystalline composites Al+Cu and Al+Mg. Fracture of the nanocrystalline composite Al+Cu occurs in an aluminum matrix, wherein the cavity formation occurs at the boundary between the grains (figure 9). Unlike the case of monocrystalline aluminum with

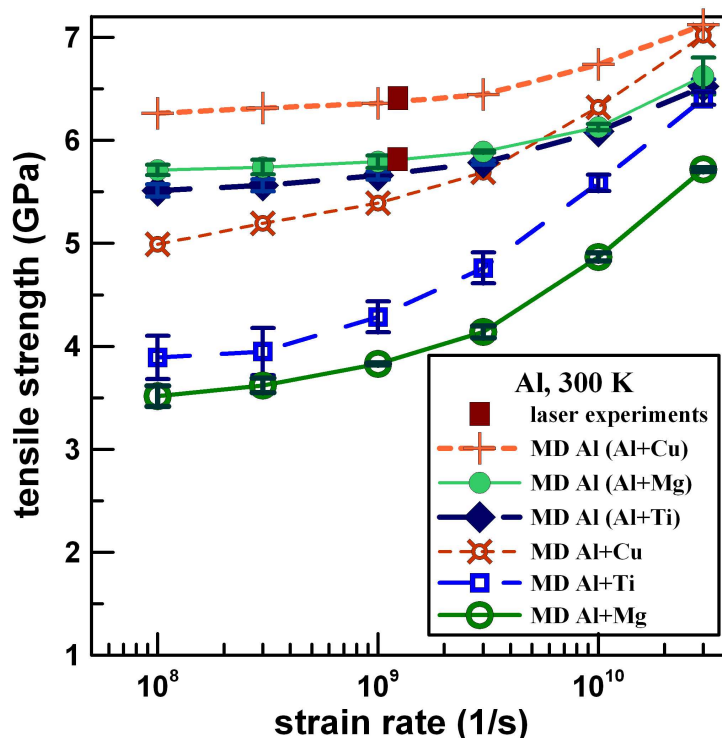


Figure 7. Strain rate dependences of tensile strength for pure Al and Al with inclusions made of Cu, Ti and Mg: uniaxial tension at the constant temperature of 300 K. Figure presents MD simulation results for pure aluminum with various potentials: “MD Al (Al+Cu)”–[8] (taken from [4]), “MD Al (Al+Mg)”–[7], “MD Al (Al+Ti)”–[6], and for aluminum with inclusions made of: copper “MD Al+Cu” (with potential [8], these results are taken from [4]), titanium “MD Al+Ti” (with potential [6]), and magnesium “MD Al+Mg” (with potential [7]). Error ranges characterize the statistical straggling and are estimated on the basis of several MD trajectories. Symbols “laser experiments” present the experimental data [11] on intensive ultra-short laser irradiation of thin Al foils.

copper inclusion, fracture does not start near the boundary of the copper inclusion; fracture begins in any point of the nanocrystalline matrix from the grain boundaries. The tensile strength of nanocrystalline composite Al+Cu determined by the tensile strength of nanocrystalline aluminum matrix and it is equal to 4.6 GPa (tensile strength of the monocrystalline aluminum with inclusion copper is 5.4 GPa). In the case of nanocrystalline composite with magnesium inclusion Al+Mg fracture occurs in the magnesium inclusion (figure 10). Tensile strength of the nanocrystalline composite Al+Mg is determined by the tensile strength of magnesium and it is equal to 3.5 GPa (tensile strength of the monocrystalline aluminum with the magnesium inclusion is 3.8 GPa). In this case, the effect of grain boundaries in the aluminum matrix on the tensile strength of the composite is minimal.

It should be noted that the results correspond to a large fraction of the grain boundaries about 0.1. In real materials the fraction of the grain boundaries is much smaller, so their influence on the tensile strength is also smaller.

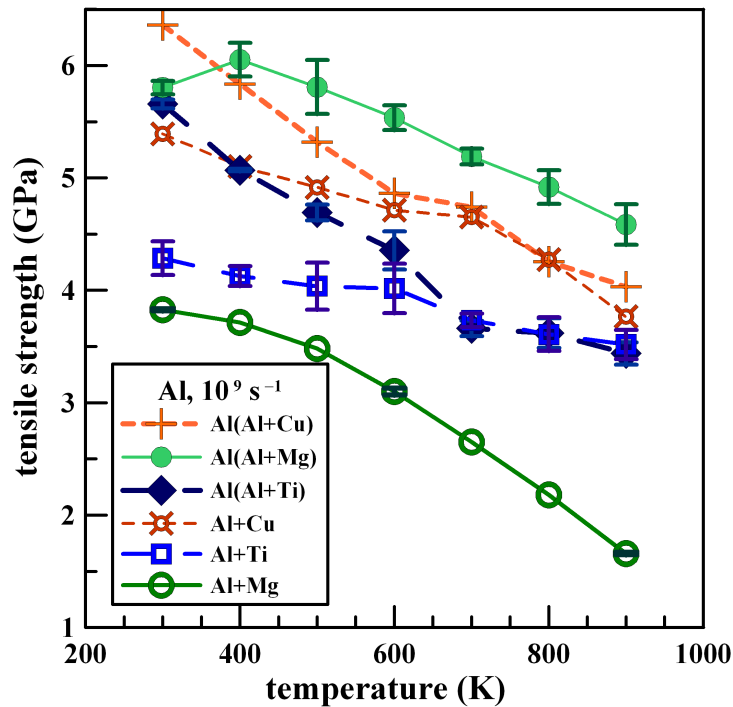


Figure 8. Temperature dependences of tensile strength of pure Al and Al with inclusions made of Cu, Ti and Mg: uniaxial tension at the constant strain rate of 10^9 s^{-1} . Figure presents MD simulation results for pure aluminum with various potentials: “MD Al (Al+Cu)”–[8] (taken from [4]), “MD Al (Al+Mg)”–[7], “MD Al (Al+Ti)”–[6], and for aluminum with inclusions made of: copper “MD Al+Cu” (with potential [8], these results are taken from [4]), titanium “MD Al+Ti” (with potential [6]), and magnesium “MD Al+Mg” (with potential [7]). Error ranges characterize the statistical straggling and are estimated on the basis of several MD trajectories.

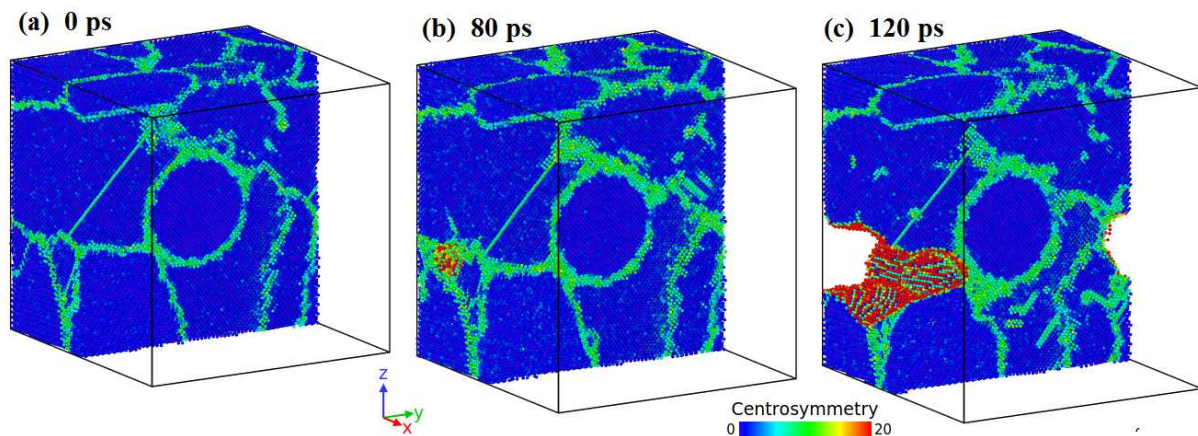


Figure 9. Distributions of centrosymmetric parameter in subsequent moments of time: tension of a nanocrystalline Al with Cu inclusion at the strain rate of 10^9 s^{-1} and temperature of 300 K. Tension is along vertical direction.

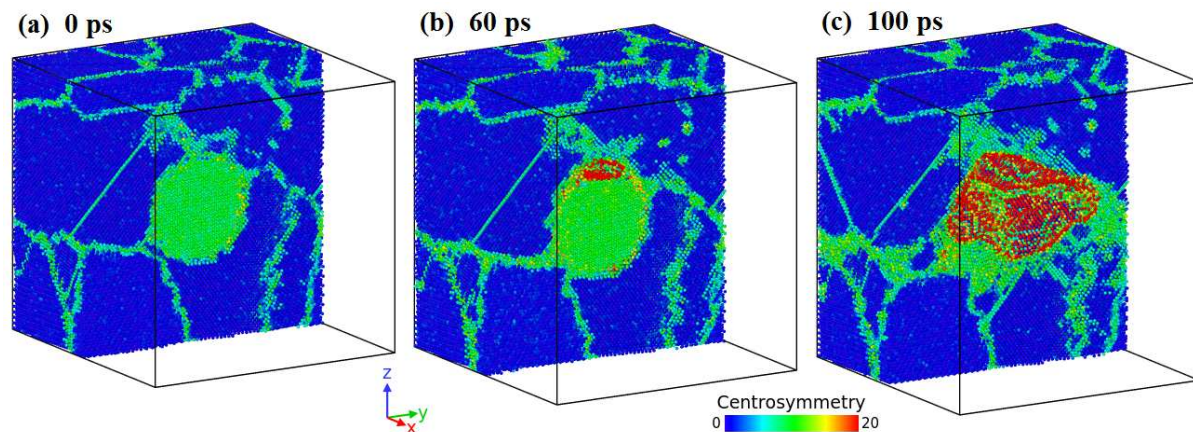


Figure 10. Distributions of centrosymmetric parameter in subsequent moments of time: tension of a nanocrystalline Al with Mg inclusion at the strain rate of 10^9 s^{-1} and temperature of 300 K. Calculations with interatomic potential [7]. Tension is along vertical direction.

4. Conclusions

With the use of MD simulations, by an example of Cu, Ti and Mg inclusions in Al matrix, we consider two different mechanisms of reduction of the tensile strength of a material with inclusions in comparison with a pure material of matrix without inclusions. The first mechanism is connected with a stress concentration in matrix near a stiff and strong inclusion (Cu and Ti). The stress concentration around the inclusion increases the local stresses to the level of the matrix strength, while the average stresses in the system are less than this level. The fracture occurs inside the matrix and does not touch the inclusion. Such mechanism is considered in [4] for the case of Cu inclusions in Al matrix, in the present work it is realized for Ti inclusions. The second mechanism acts in the case of a soft and weak inclusion (Mg), it means, the material of inclusion has lower values of elastic constants and tensile strength than the corresponding values of matrix. The fracture begins inside the inclusion and thereafter propagates into the matrix. This mechanism is realized in the case of Mg inclusions; the pressure inside it is less than the average one, and the fracture begins at a level of average pressure in the system that is higher than the strength of pure Mg.

The tensile strength of Al+Cu, Al+Ti and Al+Mg systems is calculated at varied strain rates (in the range from 0.1/ns to 30/ns at the temperature) and varied temperatures (in the range from 300 K to 900 K at the strain rate 1/ns). The rate sensitivity of strength of a material with inclusions is higher than that for a material without inclusions.

The grain boundaries in the aluminum matrix substantially reduce the tensile strength of nanocrystalline composite in the case, when fracture occurs in the matrix (nanocrystalline composite Al+Cu), and almost no effect on the tensile strength in case, when the fracture occurs within the inclusion (nanocrystalline composite Al+Mg).

Acknowledgments

This work is supported by the Russian Science Foundation (project No. 14-11-00538).

References

- [1] Chawla N and Chawla K K 2006 *Metal Matrix Composite* (New York: Springer)
- [2] Persson E L (ed) 2011 *Aluminum Alloys: Preparation, Properties and Applications* (New York: Nova Science Publishers)

- [3] Yanilkin A V, Krasnikov V S, Kuksin A Y and Mayer A E 2014 *Int. J. Plast.* **55** 94–107
- [4] Pogorelko V V and Mayer A E 2015 *Mater. Sci. Eng. A* **642** 351–359
- [5] Plimpton S 1995 *J. Comput. Phys.* **117** 1–19
- [6] Zope R R and Mishin Y 2003 *Phys. Rev. B* **68** 024102
- [7] Liu X Y, Ohotnicky P P, Adams J B, Lane Rohrer C and Hyland Jr R W 1997 *Surf. Sci.* **373** 357–370
- [8] Apostol F and Mishin Y 2011 *Phys. Rev. B* **83** 054116
- [9] Daw M S and Baskes M I 1984 *Phys. Rev. B* **29** 64436453
- [10] Stukowski A 2010 *Modell. Simmul. Mater. Sci. Eng.* **18** 015012
- [11] Ashitkov S I, Agranat M B, Kanel G I, Komarov P S and Fortov V E 2010 *JETP Lett.* **92** 516–516
- [12] Krasnikov V S and Mayer A E 2015 *Int. J. Plast.* **74** 75–91
- [13] Mayer A E and Mayer P N 2015 *JETP Lett.* **102** 89–93